



GHGT-9

Wellbore integrity analysis of a natural CO₂ producer

Walter Crow^a, Brian Williams^a, J. William Carey^b, Michael Celia^c, Sarah Gasda^d *

^aBP Alternative Energy, 501 Westlake Park Blvd., Houston Texas, 77079, USA

^bLos Alamos National Laboratory, Los Alamos, New Mexico 87545, USA

^cPrinceton University, Princeton, New Jersey, 08544

^dUniversity of North Carolina, Chapel Hill, North Carolina, 27514, USA

Elsevier use only: Received date here; revised date here; accepted date here

Abstract

The long-term integrity of wellbores in a CO₂-rich environment is a complex function of material properties and reservoir conditions including brine and rock compositions, CO₂ pressure, and formation pressure and temperature gradients. Laboratory experiments can provide essential information on rates of material reaction with CO₂. However, field data are essential for assessing the integrated effect of these factors in subsurface conditions to provide a basis for validation of numerical models of wellbore behavior.

We present a comprehensive study and conclusions from an investigation of a 30-year old well from a natural CO₂ production reservoir. The wellbore was exposed to a 96% CO₂ fluid from the time of cement placement. This site is unique for two reasons: it represents a higher, sustained concentration of CO₂ compared to enhanced oil recovery fields and the reservoir and caprocks are elastic materials that will possess less buffering capacity than carbonate reservoirs.

A sampling program resulted in the recovery of 10 side-wall cement cores extending from the reservoir through the caprock. The hydrologic, mineralogical and mechanical properties of these samples have been measured and those results are combined with an in-situ pressure-response test to investigate cement integrity over larger length scales. Fluid sampling was conducted with pressure and temperature measurements for geochemical analysis of the cemented annulus and the adjacent formation. These combined data sets provide an assessment of well integrity including original cement seal and the impacts of CO₂. Cement evaluation wireline surveys indicate good coverage and bonding, consistent with observations from sidewall cement core samples that have tight interfaces with the casing and formation. Although alteration of the cement samples is present in all cores in varying degrees, hydraulic isolation has prevented leakage based on the pressure gradient measured between the caprock and CO₂ formation. Effective cement placement was a key element to create the performance of the barrier system. Simulation of test data indicates the best match for effective permeability of the barrier is 20 micro-darcies (μ D) near the top of the caprock. The types of information collected in this survey permit analysis of individual components (casing, cement and reservoir fluid and pressure measurements) for comparison to the larger scale system including the interfaces. The results will be used as part of the CO₂ Capture Project's effort to develop a long-term predictive simulation tool to assess wellbore integrity performance in CO₂ storage sites.

© 2008 Elsevier Ltd. All rights reserved

Keywords: CO₂ Storage; well integrity; cement barrier; cement capillary pressure; effective permeability; vertical interference test; cement mineralogy

1. Introduction: Well Construction and History

This survey was conducted to determine the effect of CO₂ on the well barrier system defined as the tubulars and cement including its contact with casing and the formation. When CO₂ combines with moisture in the reservoir, carbonic acid is created which may

* Corresponding author. Tel.: +1-281-366-3801; fax: +1-281-504-2244.

E-mail address: walter.crow@bp.com.

corrode metal and Portland cement used in well construction. Fluid samples, cores and pressure response data were collected and analyzed to determine the effect on the barrier system. This information is used to provide benchmark data for modeling of the long term effects of injected CO₂ on the well system.

This survey was conducted in a well completed in the Dakota Sandstone formation found at 4561' True Vertical Depth (TVD) and had an original reservoir pressure of 1480 psi and temperature of 136 degrees F at that datum. The CO₂ in the reservoir was in supercritical phase under those conditions. This zone produces 96% CO₂ and has an average permeability of 59 millidarcies (mD), with a mineralogy that includes 69% quartz, less than 10% carbonate and water saturation of 20% based on original drill core analysis from this interval. The caprock confining layers in this well that overlie the Dakota formation are the Graneros Shale (135' vertical thickness) and Greenhorn Shale/Limestone (75' vertical thickness) formations (Figure 1.1).

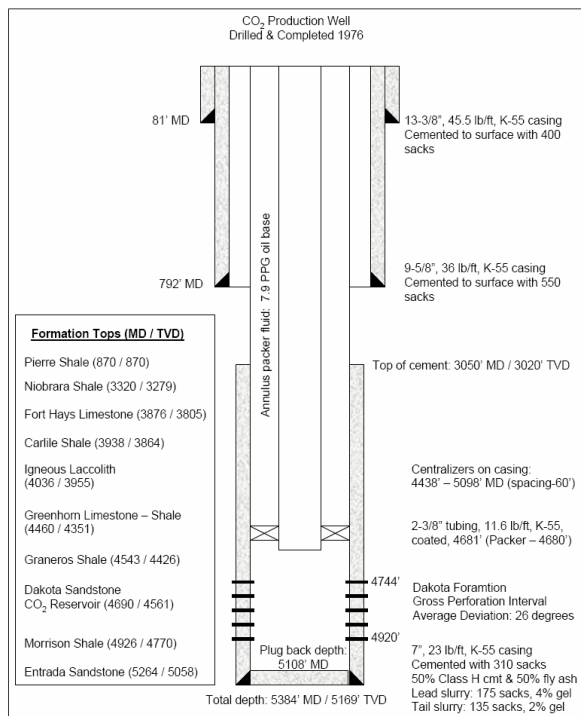


Figure 1.1: Diagram outlines the type, size and grade of tubulars used in the well construction. Production tubing was plastic-coated carbon steel and cement was portland-based with 50% fly ash.

2. Sample analysis

Soild and fluid samples were collected from outside the casing within the CO₂ reservoir and the caprock shale. Sidewall cores were cut through the casing to recover casing, cement and formation samples. Cement samples were analyzed for permeability, porosity and Young's Modulus (Fig 2.1). Cement cores taken near the CO₂ reservoir have higher average permeability (21 μD) and porosity (41%) compared to cores collected near the top of the caprock of 1 μD permeability and 25% porosity. Cement core mineralogy (Figure 2.2) determined by X-ray diffraction indicates the relative amount of original unaltered cement paste compared to the amount converted to calcium carbonate due to CO₂ exposure over the life of the well. Cement samples taken in and near the CO₂ reservoir have been almost completely converted to calcium carbonate. Samples at the top of the caprock retain more of the cement phase but have had some minimal alteration. Cement evaluation log information given by raw acoustic impedance (Fig 2.1) indicates generally good cement quality with the highest quality near the top of the shale at 4500' MD (shown by the darker brown color in the log strip). Visual observation of the cement interfaces with casing and with caprock show apparently tight contacts with no debris or other indications of porosity (Figs 2.3 and 2.4) and only very thin deposits (< 0.1 mm) of calcium carbonate (Fig 2.5). All 20 carbon steel casing samples recovered were in excellent condition with limited corrosion. Fluid samples were collected with a test tool that isolated the formation hydrostatic from the wellbore, drilled a hole through the casing, collected a fluid sample and recorded formation pressure and temperature data (Fig 2.1). The fluids had a surface-measured pH range of 5.2 to 6.1 and are slightly acidic.

The well was drilled in 1976 but production was deferred 9 years until 1985 due to pipeline availability. The well produced a total of 20 years and the first 13 years averaged 7000 standard cubic feet per day (SCF/D) of CO₂ with associated water production of 0.75 barrel per 1000 standard cubic feet. The final 7 years of production was intermittent due to increased water production. Produced water from this interval is less than 5000 parts per million total dissolved solids (TDS). There was no casing pressure observed over the 30 year life of the well. Produced water samples from the central facility indicate a range of pH 3.1 to 6.0 in recent years. The well was drilled with an oil-based mud and the barrier system consisted of 7 inch diameter casing cemented with a Portland-based system. The casing was carbon steel, K-55 grade and was centralized in the borehole. The cement was 310 sacks (391 ft³) of Class H Portland cement with 50% fly ash, 3% bentonite gel mixed at a density of 14.2 pounds per gallon (SG: 1.71). The top of the cement (behind casing) was 3050' Measured Depth (MD) which extended 1640' above the CO₂-bearing formation. The casing was pressure tested to 1000 psi for 30 minutes after a 24 hour waiting period when the estimated cement compressive strength was 2000 psi. Production tubing was plastic-coated, K-55 grade material that showed no signs of corrosion during its production life.

The measured formation pressure suggest that wellbore system provides hydraulic isolation between the CO₂ production zone and the upper caprock intervals based on the 1000 psi pressure difference across the shale.

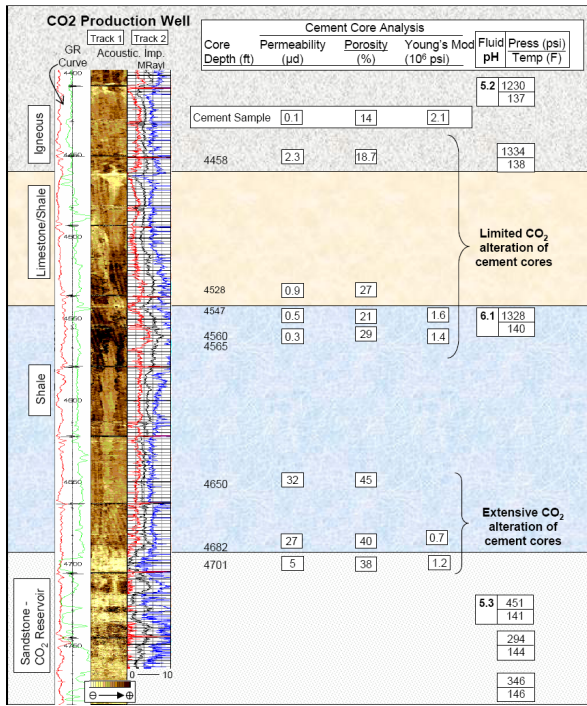


Figure 2.1: Comparison of cement core properties with pressure data and fluid pH. Raw Acoustic Impedance map from the Ultrasonic Imaging Tool provides qualitative reference of cement condition (darker = better casing-cement bond).

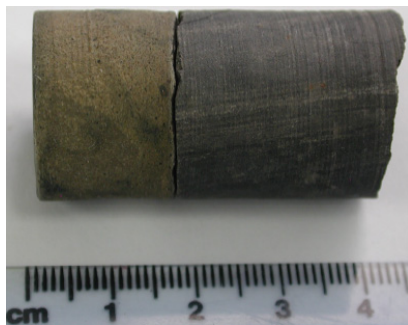


Figure 2.3: Core from 4682' of cement (left) and formation (right) to indicate a tight fit at the interface.



Figure 2.4: Core from 4650' with an intact contact between casing and cement

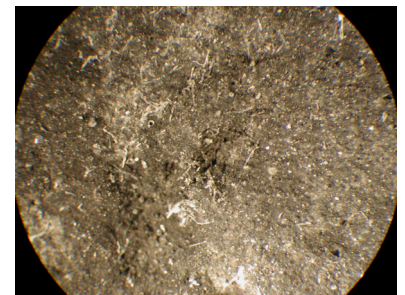


Figure 2.5: Core from 4722' in contact with the CO₂ formation has a thin layer of carbonate crystals (view is 4 mm in width).

Capillary Pressure Measurements

The capillary pressure properties of the cement cores were analyzed by centrifuge to determine the resistance to flow of a gas phase under differential pressure up to 300 psi. The estimated total pressure differential drive at the wellbore is approximately 147 psi (CO₂ buoyancy + non-hydrostatic gradient) which indicates that lab measurements cover the expected range experienced by this wellbore system.

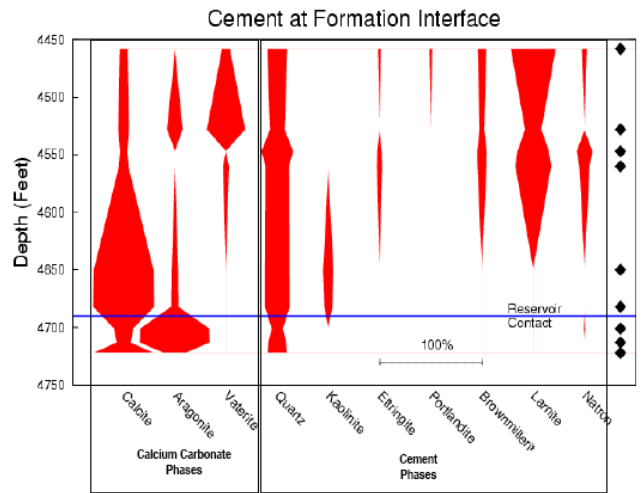


Figure 2.2: Mineralogy of cement cores to indicate the original cement phase compared to the amount of alteration to calcium carbonate. Shows most alteration in the samples from the CO₂ formation.

The capillary pressure measurements are summarized in Figure 2.3 and compared to the laboratory cement sample cured under reservoir conditions. The capillary resistance is so high for fresh, unaltered cement that air entry is not possible at pressures < 200 psi. These results suggest that for fresh cement, CO₂ penetration of the cement matrix would not occur and that diffusion is the only mechanism for CO₂ migration through the cement matrix which is extremely slow. By contrast, the relatively unaltered cement cores (shown in blue in Figure 2.3) showed that about 5% of the available pore space was accessible at pressures > 50 psi and < 300 psi. The effect of more complete carbonation further reduces the capillary resistance such that about 25% of the available pore space was accessible at pressures > 50 psi and < 300 psi. Interestingly, carbonation produces on average a small increase in capillary resistance over the relatively unaltered samples.

Years of downhole aging may have lead to the difference in capillary pressure between fresh and relatively unaltered cement. Our hypothesis is that for fresh cement, migration of CO₂ in the wellbore can only occur by passing through a defect in the barrier system (channel or cement interface transmission pathway) and alteration of the cement could only occur by diffusion of CO₂ from the defect into the cement matrix. However, it also possible that with aging of the cement, the capillary resistance decreases and a limited volume (5%) of the available pore space could be accessible by CO₂. In this case, CO₂ could invade a limited amount of the pore space if the entry pressure exceeded 50 psi. Alteration could then occur by diffusion from the 5% pore space occupied by CO₂. Once the cement has been carbonated, however, it still retains relatively high capillary resistance to CO₂. In summary, the capillary pressure measurements suggest that separate phase CO₂ migration through the cement matrix is unlikely at the pressure conditions for the wellbore.

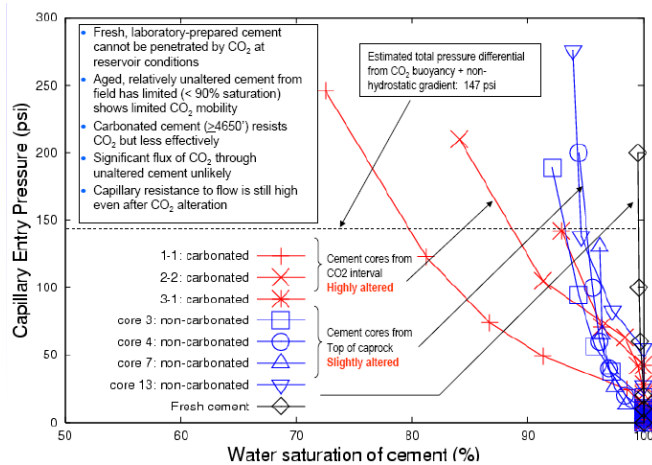


Figure 2.3: Capillary pressure properties of seven cores and a laboratory cured cement sample. The fresh cement shows great capillary resistance such that no displacement of brine was possible at air pressures < 200 psi. Estimated pressure differential at the caprock-reservoir contact of 147 psi limits capillary displacement to 20% for the most altered cores and 5% for the slightly altered cores (near the top of caprock).

3. Log Analysis

The Ultrasonic Imaging Tool (USIT) was run to provide an indication of the cement quality and its bond to the casing measured by attenuation of the acoustic signal. Log results are presented in Tracks 1 and 2 in Figure 2.1. Acoustic impedance decreases from the top of the shale to the CO₂ interval (Track 2) from 8 to 0 MRayl over the interval from 4560’ to 4700’. This general trend is consistent with a decrease in cement core hydrologic properties from the top of the caprock (1μD permeability, 25% porosity) to the CO₂ interval (21μD permeability, 41% porosity). For this well, the USIT log measurement is relatively capable of detecting differences in the quality of the cement that is attached to, and surrounding the casing (Figure 2.1).

Acoustic impedance values were plotted with porosity (Fig 3.2) and indicate a correlation between the log response and cement core alteration which has affected the hydrologic properties. This suggests that acoustic impedance can point to gross changes in porosity and are non-consistent with significant cement alteration in this well.

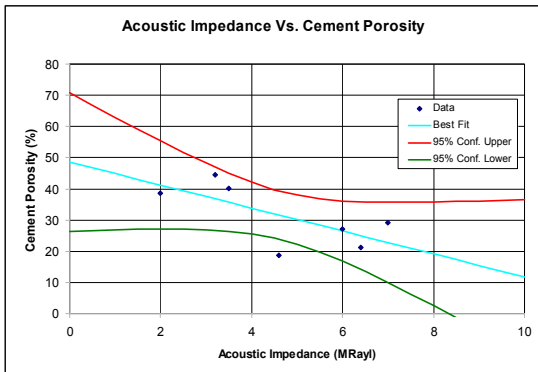


Figure 3.2: Cement Core Porosity is plotted against Acoustic Impedance log values from the depth that each core was collected. There is a general trend that suggests acoustic impedance can detect changes in porosity.

A multi-arm mechanical calliper was used to inspect the inner casing diameter and indicated minimal wall thickness loss between the perforations and packer where the casing was exposed to CO₂ and produced water. The corrosion log data is consistent with actual casing samples collected with the coring tool and showed limited or no corrosion.

There was no gas saturation evident in the caprock or other overlying layers based on results of a pulsed neutron log. This indicates no migration along the barrier system. All gas shows from the survey are in the CO₂ formation and are consistent with presence of gas from the completion.

4. Vertical Interference Test Analysis

A Vertical Interference Test (VIT) was conducted at the interface of the Greenhorn Limestone/Shale and the Graneros Shale between two perforated intervals at 4522' and 4533'. A wireline tool isolates the lower perforated interval from applied casing pressure. The applied pressure from the surface passes through the casing wall at the upper perforated zone to the cement barrier and shale interval. The pressure signal is recorded by the upper strain gauge (MRPS) and the lower quartz gauge (MRPA) adjacent to each perf interval. The results from this test indicate the extent of hydraulic communication along the exterior of the well casing between the two perforations and are a measure of the effective permeability of the wellbore system. (*Effective permeability* is defined as the average permeability of the region outside of the casing that includes the cement that was placed between the casing and the shale, the zone of shale that may have been damaged by drilling, and any annuli that may exist between the cement and the casing or the cement and the shale.)

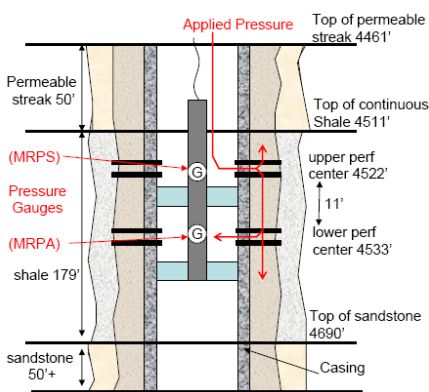


Figure 4.1: Configuration of VIT includes a wireline isolation tool with pressure gauges (MRPS & MRPA) positioned in the wellbore. The model describes perms are in a shale interval with sand (permeable) intervals above and below the shale.

A numerical model was used to simulate the VIT pressure data and determine the effective permeability. Other parameters that are tested in this simulation are permeability of the shale, the compressibility of the system, and the effective permeability of other sections of cement along the well.

The raw VIT data (shown in Figure 4.2) were normalized to a dimensionless scale between 0 and 1. On this scale, a value of 1 means that 100% of the pressure change imposed in the upper perforation is detected in the lower perforation. Likewise, a value of 0 means that no pressure change is detected in the lower perforation. The VIT data were normalized by taking the ratio of the relative pressure changes recorded in the lower and upper gauges, using Equation (4.1). An initial pressure (MRPA₀) of 1940 psi is used, which is the value recorded in the lower perforation at 5,600 seconds that corresponds to the wellbore fluid hydrostatic pressure (equivalent to a gradient of 0.439 psi/ft at 4417' TVD). Similarly, the relative pressure change in the upper perforation is the average

sustained pressure (2725 psi) minus $MRPA_0$. Since the perforations are so close together, this is an appropriate approximation. The normalization formula is as follows:

$$MRPA_{norm} = \frac{MRPA(t) - MRPA_0}{2725 - MRPA_0} \tag{Equation 4.1}$$

Governing Equation

The governing equation for this system is the continuity equation for compressible flow of a single fluid in porous media,

$$c_f \frac{\partial p}{\partial t} - \nabla \cdot \frac{k}{\mu} (\nabla p - \rho \mathbf{g}) = 0. \tag{Equation 4.2}$$

In the above equation, c_f is the compressibility, p is the fluid pressure, k is the permeability, μ is the fluid viscosity, ρ is the fluid density, and \mathbf{g} is the gravity vector. Equation (4.2) is a transient equation that describes the evolution of pressure in space and time. For this model, compressibility and permeability can vary, but the fluid viscosity and density are assumed to be constant in the near-well environment.

In Equation (4.2), the pressure response depends on the ratio k/c_f (permeability to compressibility) at each point in space. A set of values is chosen for k and c_f at each point in space. Thus, although the focus of the modelling is on permeability, the dependency on compressibility is implied.

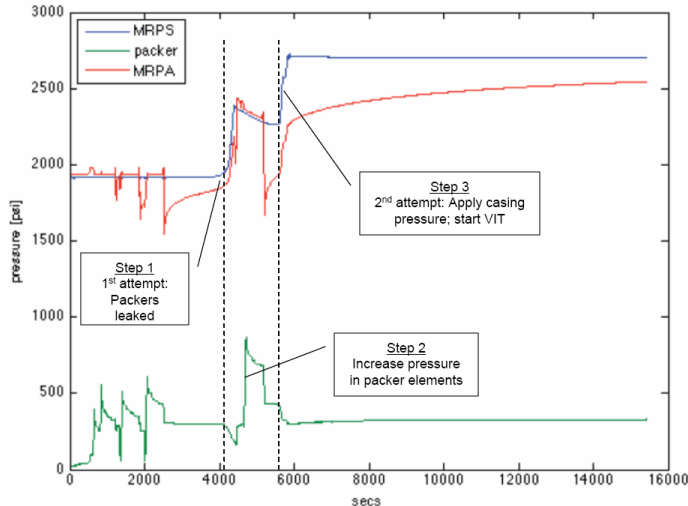


Figure 4.2: Raw data from VIT showing pressure in three gauges, MRPS in the upper perforation, MRPA in the lower perforation and the packer inflation pressure. There are two attempts to pressurize the well. The first attempt began at 4,500 s and failed due to leakage around the packers. The second attempt to pressurize began at 5,600 s and continues until the end of the test at around 15,000 s.

Numerical Method

A numerical model was developed that solves the governing equations for compressible flow of a single fluid in porous media in space and time. This model solves the system in a radially-symmetric coordinate system. The domain of interest consists of two sandstone formations separated by a low-permeability shale layer. The dimensions of the domain are 256’ in the vertical and 27,000’ in the radial direction. The inner boundary of the domain coincides with the outer casing radius (OD) and is impermeable to flow. At the outer boundary, a hydrostatic pressure condition is imposed. The top and bottom boundaries of the domain are also impervious to flow. The permeability values of the sandstone formations are assumed to be 0.1 Darcy. Initially, we assume that the shale layer is impermeable to flow.

The distance from the outer radius of the casing to the inner wall of the borehole is 1.75 in. This region corresponds to the ‘disturbed zone’ as discussed above. We assume that the shale outside this zone is undamaged for this system. For simplicity, we will refer to the effective permeability of the disturbed zone as the *cement permeability*. Although it is emphasized that the term “a

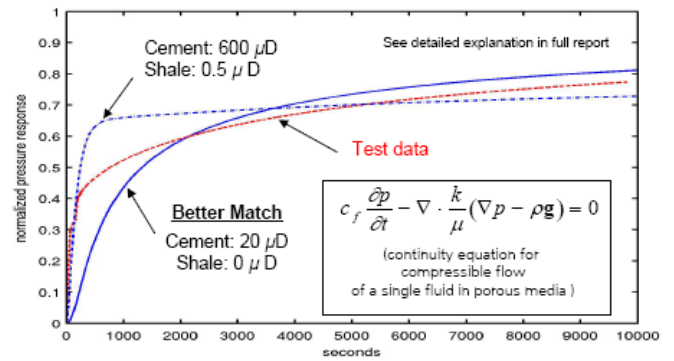


Figure 4.3: Comparison of VIT data (red dashed line) with two simulated results: (1) impermeable shale and a cement permeability of 20 μ D (blue solid line); and (2) a shale permeability of 0.5 μ D and a cement permeability of 0.6 mD (blue dash-dot line).

permeable cement” could mean the cement itself has been degraded and the flowpath is through the cement. Alternatively, it could mean that annuli are present along interfaces and flow is around the cement more than through the cement itself.

Method of analysis

In this analysis, different simulations were performed with different values of cement permeability assigned to the vertical section between the upper and lower perforations. In addition, the cement permeability may also be different in other sections along the wellbore, i.e. above the upper perforation and below the lower perforation. In this analysis, we tested numerous configurations of cement permeability and shale permeability to determine the configuration that has the best match to the VIT data. We will discuss two cases with the best fit to the data: one for an impermeable shale and one for a permeable shale.

As discussed above, the compressibility of the system is also a factor in the system response in the VIT. This means that from our discussion about Equation (4.1), we are testing not only the effect of changing the permeability but changing the ratio k/c_f . The cement compressibility was measured to be $c_f=6.38 \times 10^{-10}$ m²/N (1 m²/N = 1 Pa⁻¹ = 6,895 psi). For reference, the compressibility of water is 4.6×10^{-10} m²/N. In this analysis, we assume that compressibility in the shale is the same as the cement.

Results

In the following sections, we summarize the results of the simulated VIT performed for this analysis. For each case, the simulated data is plotted in blue along with the VIT data in red. The time axis is scaled so that time $t=0$ corresponds to the start of the VIT when the well is pressurized, which occurs at 5,600s in Figure 4.2.

Impermeable shale

We tested the case with an impermeable shale and a single value of cement permeability that is constant along the entire wellbore, extending from 10' above the upper perforation to 155' below the lower perforation. In this case, the best match to the VIT data is a cement permeability of 20 μ D (Figure 4.3, solid line). This configuration compares well with the VIT in the latter part of the transient curve (> 2000 s). The sharp increase in pressure at early time is not captured well in this case.

Permeable shale

For the case where the caprock permeability is set to 0.5 μ D, we find that a 0.6-mD cement best matches the VIT data (see Figure 4.3, dash-dot line). The cement permeability is higher in this case, which is to account for a large portion of the signal that is lost through the permeable caprock. In comparison with the VIT curve, there is a better match at early time, but at later times, the slope of the curve in this case is much flatter than the VIT curve.

Discussion and Conclusion of VIT

To summarize: for a shale that is impermeable, the best fit to the VIT data is with a cement permeability of 20 μ D; for a permeable shale (0.5 μ D), the best fit is a 0.6-mD cement. In both of these cases, the best fit was obtained for a configuration where the cement permeability is the same everywhere in the ‘disturbed zone’ that lies within the shale.

The main conclusion from this analysis is that the ‘disturbed zone’ outside of the well casing in the interval between the upper and lower perforation has an effective permeability in the range between 10 μ D and 1 mD. The cement core collected from 4528' MD had a matrix permeability of 0.9- μ D and thus the VIT data is 1 to 2 orders of magnitude greater than cement core. The enhanced permeability observed in the VIT is likely due to communication at the interfaces and thus the most likely path of any CO₂ migration would be these interfaces. We find that there is a slightly better fit to the VIT data when the shale is impermeable because the slope of the curves matches better at later times. Thus the preferred effective permeability is closer to the upper end of the estimated range (near 10 μ D).

5. Conclusions

The primary conclusions from this investigation are:

- a. The barrier system in this well appears to provide hydraulic isolation across the caprock based on formation pressure measurements made during this survey.
- b. Cement carbonation has been observed in varying degrees in cores from this well. Carbonation of cement increased permeability, porosity and had a mixed effect on capillary properties with a small increase in capillary entry pressure accompanied by an increase in the fraction of pore water displaced. It decreased the compressive strength but the cement still provides an effective barrier. These changes, while not improvements, do not result in a significant loss of cement resistance to CO₂ migration.
- c. The casing is in very good condition, consistent with good cement coverage and limited circulation of reservoir fluids along the casing-cement interface.
- d. Cement interfaces with casing and formation appear to be tight and do not have significant calcium carbonate deposition.
- e. The effective permeability of the barrier system including the cement interfaces was evaluated by numerical modelling of the VIT data, which is the preferred method to analyze in-situ migration potential. The permeability calculations from the VIT data are 1 to 2 orders of magnitude greater than the cement core permeability. This indicates that the cement interfaces with casing and/or formation are the primary path for CO₂ migration as shown by cement carbonation.
- f. Our interpretation of the data suggests that the CO₂ that has caused carbonation of cement and acidification of fluids adjacent to the caprock originated in the CO₂ reservoir (Dakota formation) and migrated along defects (primarily cement-caprock and cement-formation interfaces) within the wellbore system.
- g. Current technologies can be used to determine barrier condition. Logging results from this survey correlate with the performance measurement of the large scale vertical interference test (VIT) and the small scale cement core properties.
- h. Based on the results of the surveys in this well, conventional cement-fly ash systems can inhibit CO₂ migration even after carbonation of the cement because permeability remains relatively low and capillary resistance relatively high. The cement interfaces with the casing and formation are the areas of greatest concern for barrier system integrity; however these interfaces appear to provide sufficient flow restriction between formations in this well based on the VIT results, the lack of corrosion in the well, and the lack of sustained casing pressure.

Evidence from the subject investigation suggests that Portland-based cement systems can be used effectively in creating suitable barrier systems for long-term CO₂ storage operations, if good practices are employed during well construction. Examples of required good practices include: centralization of casing and efficient borehole mud removal for cement placement.

Acknowledgements

The authors thank the management of Carbon Capture Project Phase 2 member companies for support of this project. CCP2 member companies are: BP Alternative Energy, Chevron, ConocoPhillips, Eni, StatoilHydro, Petrobras, Shell Global Solutions US Inc. and Suncor Energy Inc. The conclusions in this report are those of the authors and are not necessarily the view of the other member companies.

Special thanks to Charles Christopher, BP Alternative Energy, for the guidance in creating this comprehensive program. Special thanks also to Ray Wydrinski, BP America for support with log analysis. Special thanks also to Andrew Duguid, Ph.D., and Matteo Loizzo of Schlumberger Carbon Services for their support in this project.